# Energy-transfer mechanisms in the KCl:$Eu^{2+}$,$Mn^{2+}$ system

R. Capelletti and M. Manfredi
*Dipartimento di Física dell'Università, Gruppo Nazionale di Struttura della Materia del Consiglio Nazionale delle Ricerche, and Centro Interuniversitario di Struttura della Materia, via M. D'Azeglio 85, Parma, Italy*

R. Cywiński, J. Z. Damm, and E. Mugeński
*Institute for Low Temperature and Structure Research, Polish Academy of Sciences, P.O. Box 937, Wrocław, Poland*

M. Solzi
*Maspec Laboratory, Parma, Italy*

(Received 3 February 1987; revised manuscript received 18 May 1987)

Energy-transfer mechanisms have been examined in the KCl:$Eu^{2+}$,$Mn^{2+}$ system at low Eu- and Mn-ion concentrations. The Eu ions represent the donor system, the Mn ions the acceptor one. No transfer evidence has been found in quenched samples; by annealing the samples at temperatures higher than 200 °C, the typical $Mn^{2+}$ emission is observed after excitation in the $Eu^{2+}$ absorption band. The energy-transfer mechanisms have been examined along the aggregation process induced by annealing the KCl:$Eu^{2+}$,$Mn^{2+}$ samples at 225 °C for very long times: three different types of behavior have been evidenced. In the early annealing stages a single pair donor-acceptor transfer mechanism is observed, while at longer annealing times an energy diffusion in the donor system, followed by a phonon-assisted transfer, takes place. Finally, at very long annealing times the energy diffusion process is followed by a resonant transfer mechanism.

## I. INTRODUCTION

As is known, the energy-transfer process consists of an interaction mechanism between centers, called donors and acceptors; as a consequence of this interaction the donor system, raised by an external source to the excited state, can release part of the absorbed energy to the acceptor system. Donor centers can act as the constituents of the host lattice. Förster[1] and Dexter[2] developed the first theories for the process in the case of multipolar coupling; Inokuti and Hirayama[3] considered the case of exchange coupling too. Mijakawa and Dexter[4] considered the possibility of the interaction of the energy involved in the transfer with the lattice phonons. Depending on the concentration and distribution of the donors and acceptors it is possible to obtain a direct energy transfer; that is, a single-step process, or more complex behavior, in which the excitation is migrating through the lattice following a multistep process before the transfer takes place.[5,6]

In the present paper the energy-transfer processes are analyzed in the system KCl:$Eu^{2+}$,$Mn^{2+}$; the donor system is represented by $Eu^{2+}$ ions, the acceptor one by $Mn^{2+}$ ions.

Optical absorption, excitation, luminescence, and luminescence time decay spectra measurements were performed on this system and compared with the same spectra measurements performed on the KCl:$Eu^{2+}$ system in order to examine the difference introduced in KCl:$Eu^{2+}$,$Mn^{2+}$ samples by the transfer processes.

Since the distance among the impurities is of extreme importance in the transfer process, the disappearing of isolated defects in the solid solution was monitored by the ionic thermocurrent technique[7] (ITC) in order to check the aggregation behavior of the impurities. For the sake of brevity, the analysis of the KCl:$Eu^{2+}$ system will not be reported here; only the results necessary for the comparison with the behavior of the KCl:$Eu^{2+}$,$Mn^{2+}$ samples and for determining the transfer rates are reported in this paper.

It is known that the KCl:$Eu^{2+}$ system is characterized by two absorptions bands lying in the ultraviolet region and by a unique emission band centered at 419 nm when the samples are quenched, namely when the Eu ions are completely dissolved in the matrix in the form of impurity-vacancy (IV) dipoles. By annealing KCl:$Eu^{2+}$ samples at room temperature (RT) and at higher temperatures,[8,9] new emission bands centered at 427, 439, and 478 nm develop.

KCl:$Mn^{2+}$ is characterized by a series of absorption bands[10,11] (that can be detected for very large $Mn^{2+}$ concentrations due to the low oscillator strength of the absorption transition) and by an emission band peaking at about 580 nm.[12] Two absorption bands of $Mn^{2+}$ ions[10,11]—that represent the acceptor system—are peaked at about 419 and 440 nm (at RT), which overlap the emission band of $Eu^{2+}$ dipoles and $Eu^{2+}$ aggregates centered at 419, 427, and 439 nm, respectively; this overlapping matches one of the conditions for the energy transfer. It is therefore possible to analyze transfer mechanisms in the $Eu^{2+}$-$Mn^{2+}$ system both when the impurities are dissolved in the matrix as IV dipoles and when the impurities form aggregates.

 

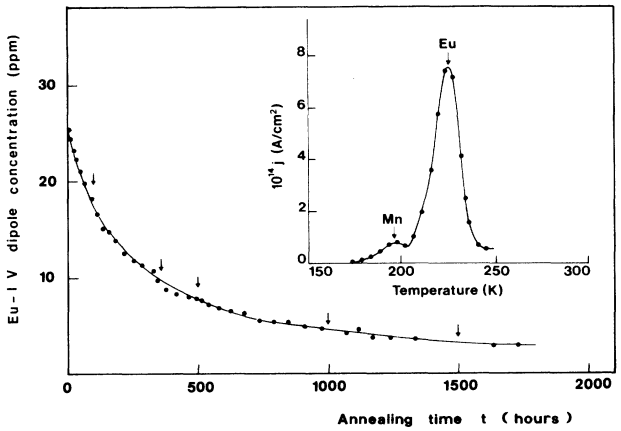


FIG. 1. KCl:$Eu^{2+}$(54 ppm),$Mn^{2+}$(3 ppm): Eu-IV dipole concentration vs annealing time at 225 °C, after sample quenching from 500 °C. Solid circles: experimental data. Solid line: calculated decay curve according a monomolecular second-order kinetics. The arrows indicate the steps at which the analysis of possible energy-transfer processes has been studied in detail. In the inset we show an ITC plot of the same sample freshly quenched: Mn-IV and Eu-IV dipole peaks are indicated.

## II. EXPERIMENTAL PROCEDURE

Single crystals of KCl:$Eu^{2+}$,$Mn^{2+}$ were grown using the Bridgman technique and the amount of $OH^-$ was minimized according to a procedure described elsewhere.[13] The actual $Eu^{2+}$ concentration in the samples was evaluated from the optical-absorption spectra at RT following the criterion reported by Suszyńska *et al.*[14]

The $Mn^{2+}$ concentration could not be evaluated by means of optical measurements due to its undetectable optical absorption. Hence the $Mn^{2+}$ concentration (in the form of IV dipoles) has been measured using the ITC technique,[7] since the ITC peak due to Mn-IV dipoles is distinct from that due to Eu-IV dipoles (see, for example, the inset of Fig. 1).

Optical-absorption spectra were gathered using a Varian 2390 recording spectrophotometer. For the emission- and excitation-spectra measurements a continuous deuterium lamp was employed as the excitation source; the luminescence was detected by means of a single-photon–counting technique. The input and output wavelengths were selected by means of a Jarrel-Ash (0.25 m) and a Jobin-Yvon monochromator. For time-resolved spectroscopy a homemade flash lamp or an Edinburgh tyrathron gated flashlamp (model 199 F) and a time-correlated single-phonon–counting technique were used. Finally, ITC spectra—gathered in order to obtain information on the aggregation of the impurities—were acquired via the usual procedure.[7]

## III. EXPERIMENTAL RESULTS

In this paper the energy-transfer processes have been examined at different stages of the aggregation in the system KCl:$Eu^{2+}$,$Mn^{2+}$ by measuring—as previously outlined—the optical absorption, excitation, luminescence, and luminescence time decay spectra. Furthermore, the IV dipole concentration has been monitored during the aggregation process in order to establish the nature of the clusters, i.e., the first aggregation products, by means of the ITC technique (see, for example, Fig. 1).

In the following we are describing—for the sake of example—the behavior of KCl:$Eu^{2+}$,$Mn^{2+}$ samples, the Eu-IV dipole concentration of which, measured immediately after a quenching, turned out to be 54 ppm. The Mn-IV dipole concentration turned out to be 3 ppm. Furthermore, KCl:$Eu^{2+}$ samples have been examined, with a Eu-IV dipole concentration ranging between 20 and 90 ppm, in order to match the $Eu^{2+}$ concentration in the double-doped samples.

### A. Quenched samples

Figure 2 shows the absorption, excitation, and emission spectra of the KCl:$Eu^{2+}$,$Mn^{2+}$ sample immediately after a fast quenching from 500 °C; only the absorption and emission bands typical of $Eu^{2+}$ dipoles are observed, evidence being present neither for absorption nor for emission of the $Mn^{2+}$ system.

### B. Evidence for Eu → Mn transfer: Emission, absorption, and excitation spectra

By annealing the samples at temperatures higher than 200 °C, the typical $Mn^{2+}$ emission, centered at about 580 nm, starts to be detectable and its intensity increases by increasing the annealing time $t_a$. In Fig. 3 the emission band of the KCl:$Eu^{2+}$,$Mn^{2+}$ system, after 360 h annealing at 225 °C, is presented as an example: Curve *a* refers to the emission detected at RT and curve *b* to that detected at liquid-nitrogen temperature (LNT). The $Eu^{2+}$ emission, shown in Fig. 3, is built up by the 419-nm emission band (related to isolated IV dipoles) and by a tail at longer wavelengths which is due to $Eu^{2+}$ aggregates.[9]

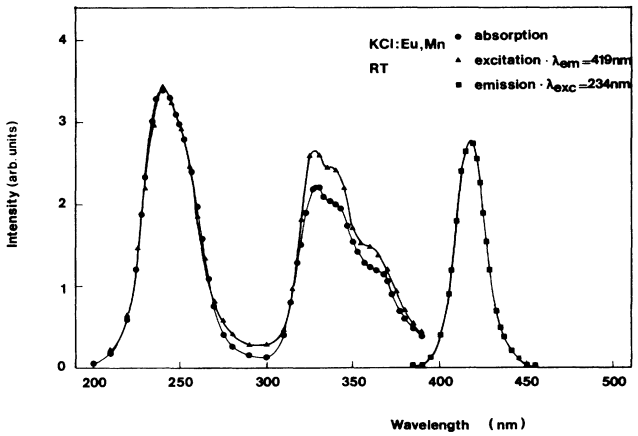


FIG. 2. Absorption (solid circles), excitation (triangles), and emission (squares) spectra of a quenched KCl:$Eu^{2+}$,$Mn^{2+}$ sample at RT, with a Eu concentration of 54 ppm and a Mn concentration of 3 ppm.

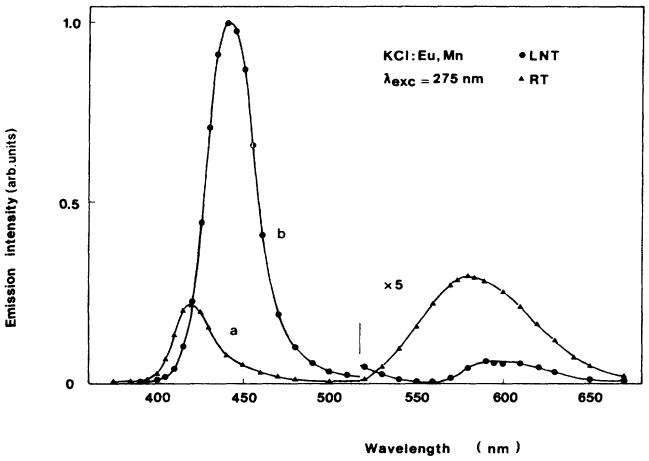


FIG. 3. Emission spectra of the KCl:$Eu^{2+}$,$Mn^{2+}$ system at RT (curve *a*) and at LNT (curve *b*) excited in the $Eu^{2+}$ absorption band; $\lambda_{exc}=275$ nm. The sample has been annealed for 360 h at 225 °C. The Eu and Mn concentrations are the same as in Fig. 1.

The tail intensity increases with the annealing time at 225 °C. Furthermore, in the 580-nm region the $Mn^{2+}$ emission is evidenced.

Figure 4 shows the emission of a KCl:$Eu^{2+}$ sample with 90-ppm $Eu^{2+}$ concentration, submitted to the same thermal treatment as the KCl:$Eu^{2+}$,$Mn^{2+}$ sample to which Fig. 3 refers. KCl:$Eu^{2+}$ samples with a $Eu^{2+}$ concentration lower than 90 ppm show the same behavior as that reported in Fig. 4. In the inset of Fig. 4, curves *a* and *b* represent—after normalization—the emissions at RT of the KCl:$Eu^{2+}$,$Mn^{2+}$ and KCl:$Eu^{2+}$ systems, respectively. The difference between them is indicative of the energy transfer which occurs, in KCl:$Eu^{2+}$,$Mn^{2+}$ samples, from $Eu^{2+}$ to $Mn^{2+}$ ions. This difference is larger in the (430–460)-nm region, indicating that at these wavelengths the transfer from $Eu^{2+}$ to $Mn^{2+}$ is more efficient. Hence this region has been examined in more detail in order to analyze the transfer mechanisms.

During the thermal-annealing process, the absorption band and excitation spectrum have been examined for the KCl:$Eu^{2+}$,$Mn^{2+}$ system. In Fig. 5 the absorption band and the excitation spectra for the emissions centered at 450 and 580 nm, respectively, are reported. The two excitation spectra overlap rather well and this fact is a further evidence of Eu-Mn transfer between the (430–460)-nm emission of the Eu system and the 440-nm absorption band of the Mn system.

The data reported in Fig. 5 have been taken for the same sample and under the same conditions of thermal annealing in which the measurements of Fig. 3 were performed. It is worth stressing that the excitation spectra related to the emission centered at 419 nm exhibit a behavior completely different from that reported in Fig. 5, but similar to that reported in Fig. 2. For the sake of brevity these latter data are not shown here.

### C. Luminescence time decay of the donor system and transfer mechanisms

The luminescence time decays have been investigated both in KCl:$Eu^{2+}$ and in KCl:$Eu^{2+}$,$Mn^{2+}$ systems, subjected to the same thermal treatments (at 225 °C), at some points along the aggregation process, namely at the initial stage ($t_a \sim 94$ h, when the $Mn^{2+}$ emission starts to be detectable), an intermediate stage ($t_a \sim 360$–$500$ h, when the $Mn^{2+}$ emission intensity at RT ranges between 0.05% and 0.1% of the 455-nm $Eu^{2+}$ emission intensity), and a final stage ($t_a \sim 1000$ h, when the emission intensities of $Mn^{2+}$ at 580 nm and of $Eu^{2+}$ at 455 nm are comparable).

The results can be summarized as follows.

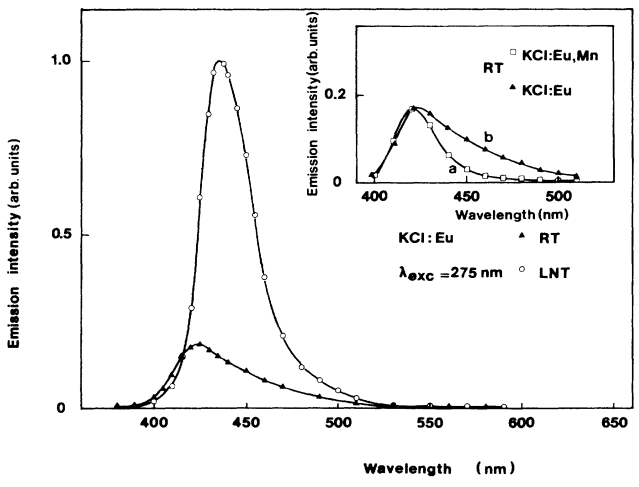


FIG. 4. Emission spectra of the KCl:$Eu^{2+}$ sample (Eu concentration of 90 ppm) at RT (triangles) and at LNT (open circles). $\lambda_{exc}=275$ nm. In the inset the emission spectra at RT of the KCl:$Eu^{2+}$,$Mn^{2+}$ (curve *a*) and KCl:$Eu^{2+}$ (curve *b*) samples are reported after normalization.

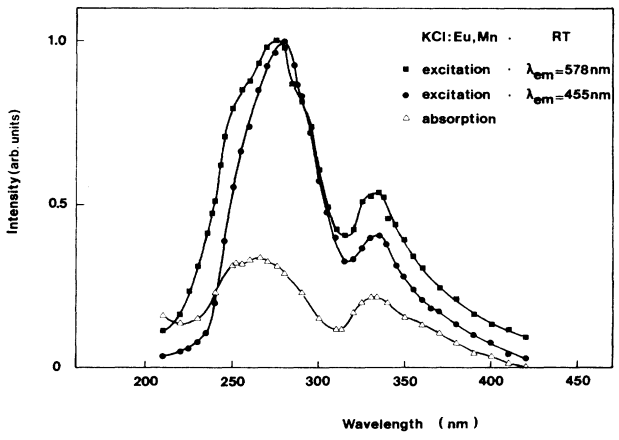


FIG. 5. Absorption band (triangles) of a KCl:$Eu^{2+}$,$Mn^{2+}$ sample (Eu concentration of 54 ppm, Mn concentration of 3 ppm) after 360 h of annealing at 225 °C. The solid circles and the squares represent the excitation spectra for the $Eu^{2+}$ and $Mn^{2+}$ emission bands, respectively.

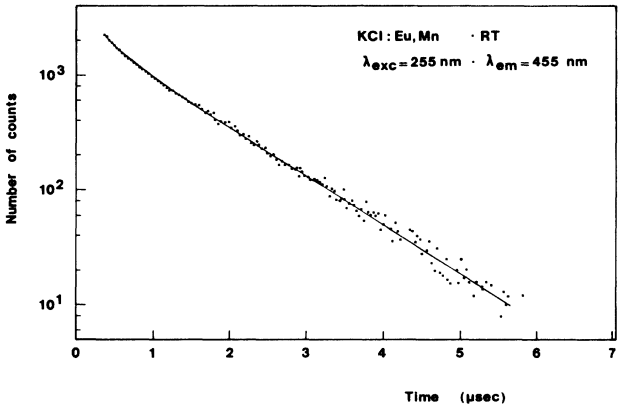


FIG. 6. Luminescence time decay signal at RT for a KCl:$Eu^{2+}$,$Mn^{2+}$ sample after 94 h of annealing at 225 °C (Eu and Mn concentrations are the same as in Fig. 1). The solid line represents the best fitting of the experimental points as explained in the text; one channel = 16 ns.

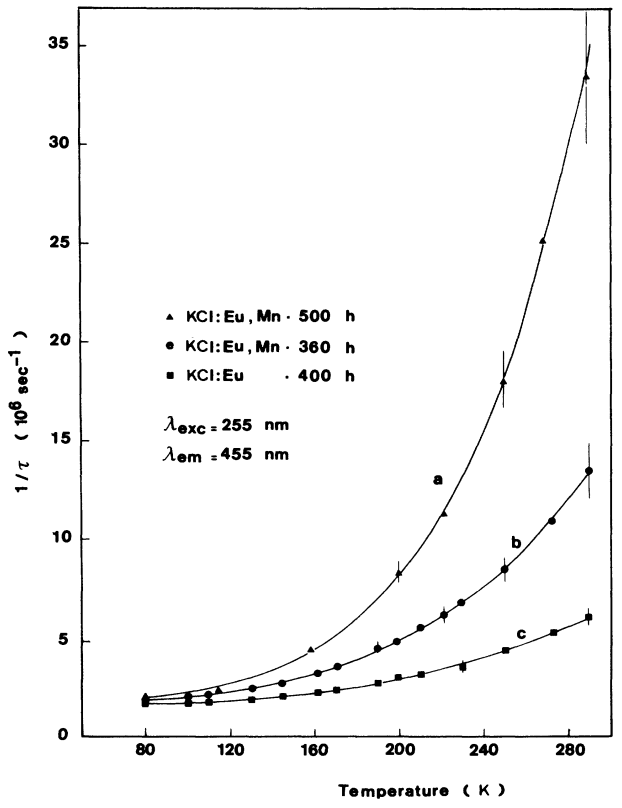


FIG. 7. Luminescence time decay rates as a function of the temperature in the range 80–295 K for the KCl:$Eu^{2+}$,$Mn^{2+}$ system after 360 h of annealing (curve *b*) and after 500 h of annealing (curve *a*), and for the KCl:$Eu^{2+}$ system after 400 h of annealing (curve *c*). $T_{anneal} = 225$ °. The solid lines represent only a guide for eyes.

(a) *Initial stage.* Figure 6 shows the time decay of the luminescence of KCl:$Eu^{2+}$,$Mn^{2+}$ detected at 455 nm. The signal is characterized by a nonexponential initial trend followed by a pure exponential behavior with a time constant typical of the early $Eu^{2+}$ aggregates as measured in KCl:$Eu^{2+}$ annealed for the same time. Figure 6 refers to a situation in which 72% of Eu-IV dipoles are still in solid solution.

(b) *Intermediate stage.* In this case the time decay signals of the KCl:$Eu^{2+}$,$Mn^{2+}$ system are characterized by a unique exponential behavior; they are not reported here for the sake of brevity. Figure 7 reports the values of the time decay rates for the KCl:$Eu^{2+}$,$Mn^{2+}$ system as a function of temperature for $t_a \sim 360$ (solid circles) and 500 h (triangles). The squares represent the values of the time decay rates of a KCl:$Eu^{2+}$ sample; it should be remarked that the behavior of KCl:$Eu^{2+}$ remains the same for annealing times ranging between 200 and 1000 h. Figure 7 refers to situations in which the Eu-IV dipole fraction, still in solid solution, is 38% and 31%, respectively.

(c) *Final stage.* In this region the Eu-IV dipole concentration is reduced to 18% of the initial value. The KCl:$Eu^{2+}$,$Mn^{2+}$ time decay values, related to the 455-nm emission, are very short and exhibit poor temperature dependence. For instance, the time decay constant ranges between 30 nsec at LNT and 24 nsec at RT; this fact suggests that—at this aggregation stage—a pure resonant transfer mechanism occurs.

## IV. DISCUSSION

Before discussion of our experimental results, let us consider the following. Recently, the transfer processes have been examined in the NaCl:$Eu^{2+}$,$Mn^{2+}$ system,[15] which, in principle, could seem very similar to the KCl:$Eu^{2+}$,$Mn^{2+}$ reported here. However, it is known that the impurity aggregation processes very often change by changing the host matrix (that is, KCl instead of NaCl) as, for example, is shown in Refs. 16 and 17. In fact, in the NaCl:$Eu^{2+}$,$Mn^{2+}$ system a very high transfer efficiency has been observed[15] and, as a consequence, the $Eu^{2+}$ emission was not detected. This fact is not observed in the KCl:$Eu^{2+}$,$Mn^{2+}$ system probably due to a different kind of Eu-Mn aggregate in which the transfer takes place. Furthermore, the ratio between Mn and Eu ranges, for the NaCl:$Eu^{2+}$,$Mn^{2+}$ system, between 100 and 5, while in our case it is 0.055. These different ratios make the NaCl:$Eu^{2+}$,$Mn^{2+}$ and KCl:$Eu^{2+}$,$Mn^{2+}$ systems different from the point of view of the transfer process.

In fact, in the former case few Eu ions are embedded in regions with many Mn ions. It is therefore reasonable that the transfer process is a single-pair process[15] from the point of view of Eu ions. In the latter case Eu aggregates probably include single Mn ions: the excitation energy can migrate in the Eu system and interact with phonons before the transfer to Mn ions takes place. As a second remark, we stress that it is practically impossible to determine the distribution of the impurities in the samples, and, in particular, the Eu and Mn distribution in the large aggregates formed as a consequence of the annealing treatments. With certain techniques, such as, for exam-

ple, the ITC technique, we are able to determine the Eu and Mn concentrations still in the solid solution; that is, in the form of IV dipoles. The energy-transfer analysis can be used just to characterize the defect distributions outlined in Ref. 15.

Concerning our experimental results, we discuss the following points.

### A. Quenched samples

As previously outlined, the $Mn^{2+}$ system is characterized by many absorption bands; among them those peaking at 419 and 440 nm strongly overlap the Eu-IV dipole emission (peaking at 419 nm) and those due to Eu aggregates (peaking at 427 and 439 nm, respectively). The absence of any $Mn^{2+}$ emission in quenched KCl:$Eu^{2+}$,$Mn^{2+}$ samples (see Fig. 1) is probably due to the large distance between $Eu^{2+}$ and $Mn^{2+}$ ions due to the low overall concentration of these impurities and to the fact that they are dispersed in the lattice. Let us estimate the value of the critical distance for $Eu^{2+}$-$Mn^{2+}$ transfer, using the current theoretical models. The energy-transfer probability in the case of a dipole-dipole interaction, $P(\mathrm{dd})$, is given by Dexter[2] and by Blasse:[18]

$$P(\mathrm{dd})=0.56\times 10^{28}\frac{Q_A}{R^6\tau_D}\frac{1}{E^4}\int f_D(E)F_A(E)dE\ , \qquad (1)$$

where $Q_A$ is related to the oscillator strength $P_A$ of the transition[15] according to $Q_A=4.8\times 10^{-16}\ P_A$, $R$ is the distance between donors and acceptors, $\tau_D$ is the decay time of donors, $f_D(E)$ and $F_A(E)$ represent, in the overlapping integral, the normalized shape of the donor emission band and the acceptor absorption band, respectively, and $E$ is the average value of the energy involved in the transition.

Usually a critical value of the distance $R_c$ is defined as the value for which the transfer probability equals the probability of intrinsic radiative emission of the donors. Namely, for $R=R_c$, we have

$$P(\mathrm{dd})\tau_D=1\ . \qquad (2)$$

We assume a value of $10^{-7}$ for $P_A$ of $Mn^{2+}$ ions (as quoted, for example, in Ref. 19) and a value of 2.82 eV for $E$. The overlapping integral is evaluated as 2 $eV^{-1}$ by using the $Mn^{2+}$ absorption band reported in Ref. 11. In fact, due to the very low $Mn^{2+}$ concentration present in our samples the related absorption bands are not detectable. From (1) and (2) it is possible to obtain, for $R_c$,

$$R_c^{\mathrm{dd}}=4.7\ \text{Å}\ .$$

In an alternative hypothesis, the transfer process can take place through an electric-dipole–quadrupole interaction. In fact, the $Mn^{2+}$ transition is partially forbidden as an electric-dipole transition.[19,20] The dipole-quadrupole transfer probability $P(\mathrm{dq})$ can be evaluated[2] and it was used in order to estimate the critical distance $R_c^{\mathrm{dq}}$ for $Eu^{2+}$-$Mn^{2+}$ transfer. We obtained a value of 29 Å. The mean distance between $Eu^{2+}$ and $Mn^{2+}$ ions in our quenched samples can be estimated to be of the order of 123 Å, a value that is considerably larger than the critical $R_c$ values previously obtained; the transfer probability is, in this case, some order of magnitude less than the intrinsic $Eu^{2+}$ decay constant $\tau_D$. Hence no $Eu^{2+}$-$Mn^{2+}$ transfer can occur in quenched samples. Furthermore, no radiative transfer (which is proportional to $R^{-2}$ rather than $R^{-6}$) (Ref. 21) has been observed, probably due to the very low oscillator strength of $Mn^{2+}$ absorption.

### B. Aggregation process: Initial stages

Let us now discuss the transfer mechanisms observed during the aggregation process. The $Mn^{2+}$ emission is easily detected (see Fig. 3) in samples annealed at 225 °C for long times. The results can be explained by means of a transfer process allowed by the overlapping between $Eu^{2+}$ aggregate emission in the range 430–460 nm and the $Mn^{2+}$ absorption centered at 440 nm, and by a reduction of the distance between $Eu^{2+}$ and $Mn^{2+}$ ions. We assume that in the early aggregation stages the donor and acceptor distribution is still random, even if the relative distances are reduced with respect to the quenched situation. For a nonradiative single-step transfer process, and in the case of electric multipolar interactions, the luminescence time decay signal of the donors is given by[3]

$$\Phi(t)=\Phi_0\exp\left[-\frac{t}{\tau_D}-\tfrac{4}{3}\pi\Gamma(1-\tfrac{3}{s})N_aR_c^3\left[\frac{t}{\tau_D}\right]^{3/s}\right]\ , \qquad (3)$$

where $s=6,8,10$ for dipole-dipole, dipole-quadrupole, and quadrupole-quadrupole interaction, respectively, $N_a$ is the acceptor concentration, $R_c$ is the critical transfer distance, and $\tau_D$ is the intrinsic donor decay rate. Equation (3) gives a typical initial nonexponential trend followed by a simple exponential decay characterized by the time constant $\tau_D$ of the donor system in the absence of the transfer channel. The donor-acceptor pairs in which the transfer takes place contribute to the initial nonexponential trend; the isolated donors, which cannot transfer the excitation, contribute to the exponential region. The experimental points of Fig. 5(a) have been fitted by means of a CERN MINUIT computer program using Eq. (3). The best fitting of the experimental results was obtained by assuming $s=6$, namely a dipole-dipole interaction.

### C. Aggregation process: Intermediate stages

In the intermediate aggregation region the luminescence time decay signal are characterized by a unique exponential. It is reasonable to assume that during the aggregation process the local concentration of $Eu^{2+}$ ions (the donors) increases around the $Mn^{2+}$ ions (the acceptors) and, as a consequence, donor-donor interactions can take place as well.

The energy diffusion among donors can be very quick, leading to a spatial equilibrium in the donor system.[5] The simple exponential decay can be accounted for because the fast diffusion can average the donor-acceptor pairs for what concerns the transfer rates. Example of simple exponential behaviors in the case of fast diffusion among donors are reported in Refs. 22 and 23.

From Eq. (1) it is possible to estimate the transfer probability between $Eu^{2+}$ ions in KCl and the critical distance in order to support the possibility of a fast energy migration. The critical distance $R_c$ for $Eu^{2+}$-$Eu^{2+}$ transfer turns out to be of the order of 22 Å, in agreement with the results of Merkle *et al.*[24] The minimum distance between $Eu^{2+}$ pairs in various kinds of possible $Eu^{2+}$ aggregates is 6.28 Å (dimer configuration).

Assuming, as an example, a mean distance of 6.28 Å between $Eu^{2+}$ ions, the transfer rate between these ions turns out to be of the order of $10^{-9}$ s. If the unique exponential slope of the time decay signals of donor luminescence is connected with the fast diffusion of the energy, the problem consists of determining the mechanism responsible for the donor-acceptor transfer that represents the ultimate stage of the energy-migration process. This transfer can be resonant or phonon assisted, depending on the matching of the energies between the transitions of donors and acceptors, respectively. One possibility of distinguishing between resonant and nonresonant mechanisms is connected to the comparison of the transfer rates, as a function of the temperature, with the available theoretical models developed for resonant[22] and nonresonant processes.[5]

The transfer rates obtained from the data of Fig. 7 are reported as a function of temperature in Fig. 8. The solid line represents the best fitting obtained by using the available theoretical models; the best fit has been obtained by assuming that the transfer probability $P(\omega,T)$ as a function of temperature is given by

$$P(\omega,T) \propto \left[ \frac{e^{\hbar\omega/k_B T}}{e^{\hbar\omega/k_B T}-1} \right]^N , \tag{4}$$

where $N$ is the number of phonons involved in the transfer process, $\hbar\omega$ is the average phonon energy needed to make up the energy mismatch $\Delta E = N\hbar\omega$, and $k_B$ is the Boltzmann constant. From the best fitting of the experimental data (solid circles, i.e., $t_a \sim 360$ h) of Fig. 7, it has been possible to determine the phonon energies $\hbar\omega$ and the parameter $N$:

$$\hbar\omega = 13.6 \text{ meV}, \quad N = 5 .$$

$\Delta E$ results in 68 meV. For the open triangles (i.e., $t_a \sim 500$ h) of Fig. 6, $\Delta E$ results in about 58 meV.

Usually the phonons contributing to the transfer process have energies close to the maximum of the phonon spectrum. Merkle *et al.*[24] report—for quenched KCl:$Eu^{2+}$—the presence of three peaks in the phonon spectrum, at 6.3, 12.5, and 24.7 meV, respectively. The last one is close to the cutoff energy and has been attributed[25] to a pseudolocalized mode due to the $Eu^{2+}$ impurity. Unfortunately, no phonon spectrum has been reported for KCl:Eu containing large aggregates.

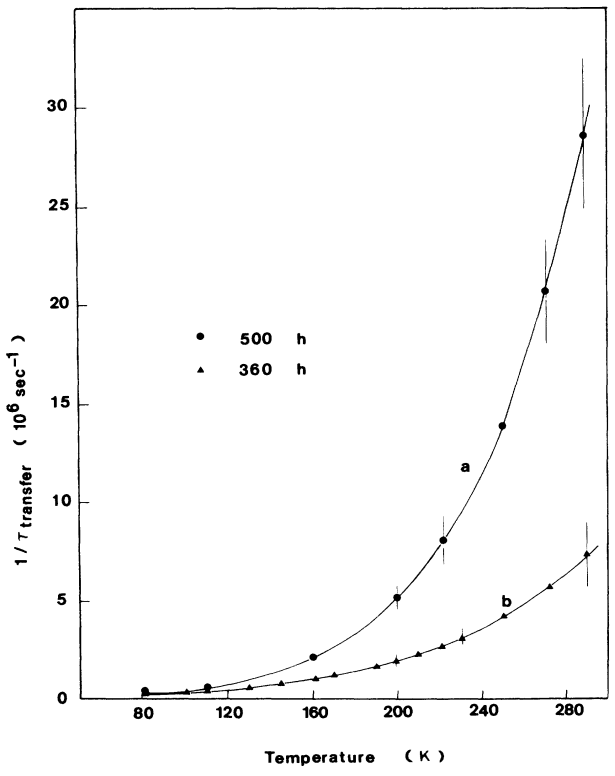


FIG. 8. Transfer rates from the decay rates reported in Fig. 7. Curves *a* and *b* have been obtained, respectively, from curves *a* and *b* of Fig. 7. The solid lines represent the best fitting, obtained by using Eq. (4), as explained in the text.

### D. Aggregation process: Final stages

In the late stages the transfer probability is practically independent of temperature. For a resonant process Gandrud and Moos[22] found, for example, that the transfer probabilities are practically equal at LNT and RT. The small changes observed in the transfer probabilities in our case can be explained as arising from small displacements, due to temperature, of the peak position of the emission and absorption bands of donors and acceptors, respectively.[5] This could result in a small reduction of the overlapping integral of the bands and, as a consequence, in a small change of the transfer probabilities.

In conclusion, the following behavior for KCl:$Eu^{2+}$,$Mn^{2+}$ system—at the concentration used and after the thermal annealings performed—can be sketched. In the quenched situation no transfer has been observed. By annealing the sample, some $Eu^{2+}$-$Mn^{2+}$ pairs assume a configuration characterized by a distance value near the critical one, and some transfer processes start to take place. In the early aggregation stages the transfer mechanism seems to be chiefly a single donor-acceptor–pair process. At longer annealing times $Eu^{2+}$ aggregates of increasing complexity are formed and characteristic of the transfer is the unique exponential decay. Phonon-assisted transfer and, finally, resonant transfer mechanisms, have been evidentiated.

The transfer mechanism between $Eu^{2+}$ and $Mn^{2+}$ ions seems sensitive to the aggregation state of the impurities; this fact suggests the possibility of using the analysis of

the energy-transfer mechanisms in order to obtain complementary information on the aggregation processes. In particular, for phonon-assisted transfer mechanisms the phonon energies obtained from the fittings of the transfer rates as a function of the temperature can give information on the structure of the phases growing around the impurity which acts as an acceptor.

[1]T. Förster, Ann. Phys. (Leipzig) **2**, 55 (1948).
[2]D. L. Dexter, J. Chem. Phys. **21**, 836 (1953).
[3]M. Inokuti and F. Hirayama, J. Chem. Phys. **43**, 1978 (1965).
[4]T. Mijakawa and D. L. Dexter, Phys. Rev. B **1**, 2961 (1970).
[5]R. C. Powell and G. Blasse, in *Structure and Bonding,* edited by J. D. Dunitz *et al.* (Springer, Berlin, 1980), Vol. 42, p. 43.
[6]M. J. Weber, Phys. Rev. B **4**, 2932 (1971).
[7]C. Bucci, R. Fieschi, and G. Guidi, Phys. Rev. **145**, 816 (1966).
[8]F. J. López, H. Murrieta S., J. Hernández A., and J. Rubio O., Phys. Rev. B **22**, 6428 (1980).
[9]J. Rubio O., H. Murrieta S., J. Hernández A., and F. J. López, Phys. Rev. B **24**, 4847 (1981).
[10]A. Mehra and P. Venkateswarlu, J. Chem. Phys. **45**, 3381 (1966).
[11]A. Mehra, Phys. Status Solidi **29**, 847 (1966).
[12]R. J. Ginther, J. Electrochem. Soc. **98**, 74 (1951).
[13]R. Voszka, I. Tarjan, L. Berkes, and J. Krajsovszky, Kristall. Tech. **1**, 423 (1966).
[14]M. Suszyńska, R. Capelletti, M. Czapelski, and A. Gainotti, in *Proceedings of the International Symposium on Ionic Crystals, 1979, Russe, Bulgaria—Scientific Reports* (Higher Institute of Machine Building, Russe, Bulgaria, 1979), Vol. XXI, p. 141.
[15]J. Rubio O., H. Murrieta, S., R. S. Powell, and W. A. Sibley, Phys. Rev. B **31**, 59 (1985).
[16]R. Capelletti and M. Manfredi, Phys. Status Solidi A **86**, 333 (1984).
[17]S. Unger and M. M. Perlman, Phys. Rev. B **10**, 3692 (1974).
[18]G. Blasse, Philips Res. Rep. **24**, 131 (1969).
[19]A. L. N. Stevels and J. M. P. J. Verstegen, J. Lumin. **14**, 207 (1976).
[20]A. L. N. Stevels and A. D. M. Schrama-de Paw, J. Electrochem. Soc. **123**, 691 (1976).
[21]T. Holstein, S. K. Lyo, and R. Orbach, Phys. Rev. B **16**, 934 (1977).
[22]W. B. Gandrud and H. W. Moos, J. Chem. Phys. **49**, 2170 (1968).
[23]D. Fay, G. Huber, and W. Lenth, Opt. Commun. **28**, 117 (1979).
[24]L. D. Merkle, R. C. Powell, and T. M. Wilson, J. Phys. C **11**, 3103 (1978).
[25]M. Wagner and W. E. Brown, Phys. Rev. **139**, A223 (1965).